APATITE-MELT VOLATILE PARTITIONING UNDER LUNAR CONDITIONS. N. J. Potts[1,2*], W. van Westrenen[2], R. Tartèse[1], I. A. Franchi[1], M. Anand[1,3]. [1]Department of Physical Sciences, The Open University, Milton Keynes, UK. (*nicola.potts@open.ac.uk). [2]Faculty of Earth and Life Sciences, VU University Amsterdam, Amsterdam, NL. [3]Department of Earth Sciences, The Natural History Museum, London, UK.

Introduction: The volatile component of apatite [$Ca_5(PO_4)_3(F,Cl,OH)$] makes it a popular choice for studying the abundance and distribution of indigenous lunar volatiles [e.g. 1-5]. The thermodynamic behavior of volatile partitioning into apatite is, however, poorly constrained. Limited experimental studies of apatite/melt partitioning have focused on terrestrial systems [6], chlorine-brine systems [7], or Martian conditions [8]. Recent studies applicable to basaltic magmas have varied parameters in each experiment [9] making it difficult to extract individual effects of temperature, pressure, and melt composition. Modeling of apatite/melt partitioning of volatiles in crystallizing melts [10] demonstrated the importance of quantifying abundances of all of the main volatiles, as they are major structural components in apatite. At present, experimentally-derived partition coefficients remain undetermined for lunar compositions and conditions.

In this study, fluorapatite, depleted in OH and Cl, was grown in equilibrium with silicate melt to provide a baseline for further experiments. These experiments were conducted with bulk compositions similar to that of late-stage mesostasis regions in Apollo lunar basalt samples [11] in which apatite is typically found. Once partitioning behavior in a nominally 'dry' fluorapatite system is constrained additional experiments will add in varying amounts of OH and Cl. The aim is to enable accurate and precise tracking of the effects of volatiles on partitioning. Once these effects are known robust back-calculations of volatile contents in lunar melts, from which apatite crystallized, could be attempted.

Methods: *Experimental methods.* Experiments were conducted in an end-loaded piston cylinder at VU University Amsterdam using a talc-pyrex assembly. For each experiment a graphite bucket was filled with starting material and closed with a graphite lid. The bucket was inserted into a triple crimped and welded Pt capsule. The double-capsule was then placed in an alumina inner tube. A $W_{97}Re_3$-$W_{75}Re_{25}$ thermocouple (T/C) was used to measure and control *T* throughout the experiment. The sample was placed in the hotspot of the assembly, 2 mm from the T/C tip end, shown to be 10 °C hotter than the T/C reading [12]. Runs were performed using a "hot piston-in" technique to achieve the desired *P-T* conditions. Each mixture was heated to 1550 °C (super liquidus) at 100 °C/minute, dwelled for 10 minutes, and subsequently cooled to final experimental temperatures at 50 °C/hr.

During the heating cycle *P* was kept low, ~300 psi, until the final *T* was reached and then increased to ~715 psi (equivalent to 1 GPa). Experiments were left to dwell for 21 hrs at final *T*. Runs were quenched by turning off the power. Experiments were conducted for 7, 18, 46, and 72 hrs to assess equilibrium.

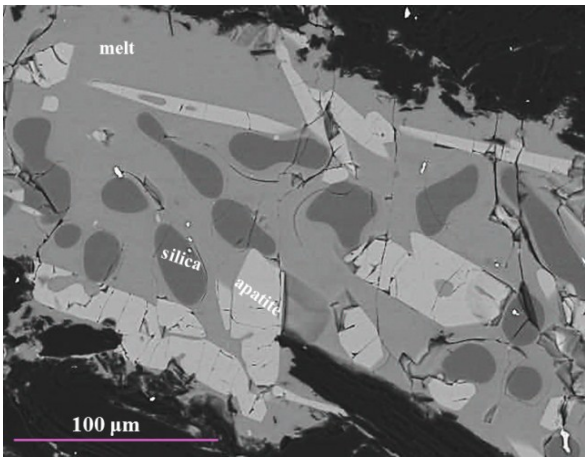

Figure 1: *Back-scattered electron (BSE) image of experimental sample with representative apatites.*

Sample imaging. Samples were imaged with The Open University FEI Quanta 3D dual beam secondary electron microscope (SEM). BSE images were acquired, using an electron beam with a 20 kV accelerating voltage and a 0.6 nA beam current.

NanoSIMS methods. Samples were coated with 30 nm of gold and were transferred into the Cameca NanoSIMS 50L, at The Open University. During analysis a 20 × 20 µm area was pre-sputtered using a ~700 pA beam for 1 minute. Apatite and glass targets were identified in these areas, using real time imaging of Si and F secondary ions. Once they were identified an 8 × 8 µm area was further rastered using a 110 pA beam for 1 minute. For analysis, secondary ions of ^{16}O ^{1}H, ^{18}O, ^{28}Si, ^{19}F, ^{31}P, and ^{37}Cl were collected simultaneously from the central area of a 4 × 4 µm area using a 30 pA beam current for 3 minutes. F, OH and Cl abundances were calibrated using $^{19}F/^{18}O$, $^{16}O^{1}H/^{18}O$ and $^{37}Cl/^{18}O$ ratios measured on apatite [13] and glass [14] standards with known volatile abundances.

Results: Temperatures in this study are higher than those in the real lunar systems due to experimental restrictions. To perform 'dry' experiments at natural temperatures (~900 °C) prohibitively long run times would be required (>>72 hrs). In our run products vol-

atile loss is observed in runs of 48 hrs and longer. Experiments at 1500 °C did not grow apatite (or any other solid phase) but instead displayed silicate liquid immiscibility. Experiments run at 1300 °C produced small (<3 µm) apatites with a small melt fraction (close to the solidus of the dry system) and were not measurable. All apatites in the measured samples were euhedral and varied in size from ~5 - 20 µm (Figure 1). Measurements were made on a variety of apatite sizes across the samples. Standard deviations on volatile abundances in apatite and glass analyses were low in-

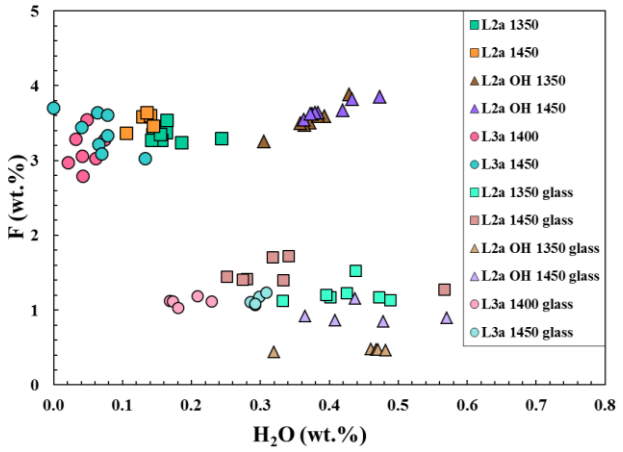

dicating homogenous, unzoned phases.

Figure 2: *F and H_2O abundances of experimental apatites and glasses. Cl abundance ~0.03 wt.% for all experiments except L2a OH 1450 with 0.19 wt.% in apatite and 0.07 wt.% glass. Error bars smaller than points.*

Initial series L2a experiments have intermediate H_2O abundances in apatites (~0.11 – 0.2 wt.%) and melt (~0.2-0.5 wt.%; Figure 2). Series L3a experiments were prepared and then stored at 110 °C for a minimum of 2 days prior to the experiment which reduced the apatite H_2O content to ~0.02 – 0.1 wt.% and melt H_2O content to ~0.1 - 0.3 wt.% (Figure 2). For the series L2a_OH experiments, 3 ml of DI water was added to the L2a powder, which was stored at 110 °C for 20 minutes then prepared. This translated into an increased H_2O content in apatite at ~0.3 - 0.5 wt.% and an increase in the melt OH content to 0.3 – 0.6 wt.%.

As discussed in previous studies [9, 10] the volatile content of apatite is a function of the availability of all three volatiles as F + Cl + OH = 1 (*apfu*) in apatite. As such, using the exchange coefficient (K_D), as defined in Equation 1, is required.

$$K_D^{F-H_2O} = \frac{\left(X_{Ap}^{F} / X_{melt}^{F}\right)}{\left(X_{Ap}^{H_2O} / X_{melt}^{H_2O}\right)} \qquad (Eq.1)$$

Similar to the experiments of [9] there appear to be no strong relationships between K_D and intrinsic variables (*T*, composition, etc.) in our experiments. Our experiments, and those of [9], appear to suggest a relation between $K_D^{Cl\text{-}H2O}$ and $K_D^{F\text{-}H2O}$, however, the lack of overlap in *P-T*-composition between the two experimental sets makes this difficult to constrain further (Figure 3). No trends for H_2O-Cl/F-Cl or H_2O-F/Cl-F are seen with experiments from this study or [9]. Large variations in K_D values are seen in Figure 3, from both experiments here and those of [9]. Variations in K_D values within both data sets are similar (factor of 10) even though experimental conditions differ. These variations are, therefore, controlled by experimental conditions.

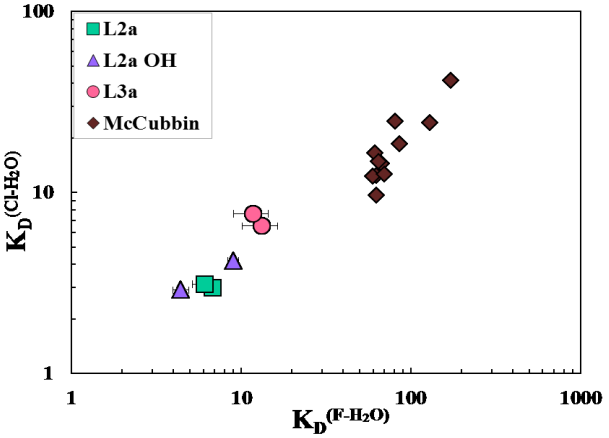

Figure 3: *$K_D^{Ap\text{-}melt}$ for F-H_2O and Cl-H_2O plotted for experiments in this study and [9].Error bars are propagated errors and generally smaller than points. No error bars given for data from [9].*

Ongoing experiments will increase the H_2O contents in the system to provide insight into whether these trends and variations continue.

Acknowledgements: This work was funded by an STFC Studentship awarded to NJP, research grant to MA (Grant no. ST/I001298/1), and a NWO Vici grant to WvW. Francis McCubbin is thanked for providing apatite standards. Thanks also to Edgar Streenstra for lab assistance.

References: [1] Boyce J.W. et al. (2010) *Nature*, *466,* 466-486. [2] McCubbin F.M. et al. (2011) *GCA, 75,* 5073-5093. [3] Greenwood, J.P. et al. (2011) *Nature Geosci., 4,* 79-82. [4] Barnes J.J. et al. (2013) *Chem. Geol., 337-338*, 48-55. [5] Tartèse R. et al. (2013) *GCA, 122*, 58-74. [6] Doherty A.L. et al. (2014) *Chem. Geol., 384, 94-109* [7] Mathez, E.A. and Webster, J.D. (2005) *GCA*, *69*, 1275-1286. [8] Vander Kaaden, K.E. et al., (2012) *LPSC XLIII,* #1247. [9] McCubbin, F.M. et al., (*in review*) *Am. Min*. [10] Boyce J.W. et al. (2014) *Science, 344,* 400-402 [11] Potts, N.J. et al. (2014) *LPSC XLIV*, #1946. [12] Watson, E. et al. (2002) *EPSL, 51,* 322-335. [13] McCubbin F.M. et al. (2012) *Geology, 40,* 683-686. [14] Jochum, K.P. et al. (2007) *GGR, 29,* 285-302.